# Monitoring of Reservoir Scale Microseismicity Using Downhole Geophone Arrays at the Utah FORGE EGS Project During Stimulation of Injector Well 16A(78)-32

**Phil Wannamaker, Ben Dyer, James Rutledge, Kristine Pankow, Dimitrios Karvounis, Falko Bethmann, Peter Meier, John McClennan and Joseph Moore**

**Energy & Geoscience Institute at the University of Utah, Geo-Energie Suisse, Santa Fe Seismic LLC, University of Utah Seismograph Stations**

**Keywords**

*EGS, Microseismicity, Geophones, Downhole, Reservoir, FORGE*

## ABSTRACT

Downhole seismic monitoring instrumentation was installed at the Utah FORGE project area in advance of the hydraulic stimulation near the toe of injector well 16A(78)-32 during April, 2022. The goal was to map and characterize the fracture systems created and activated for reservoir development through fluid injection and migration. The downhole array is a complement to shallow borehole and surface monitoring that addresses mitigation strategies for potential seismic hazards associated with injection and migration over the larger FORGE footprint. The hydraulic stimulations at FORGE included three stages over a ten-day period near the toe interval of the well drilled eastward at an angle of 65$^{o}$ to the vertical through granite, reaching a total vertical depth of 8500 ft and temperature of 220°C. Injection volumes were small, on the order of a few thousand barrels, at pressures near 7000 psi, and with rates of several tens of barrels per minute. The first injection was applied by pressurizing the entire open hole section below the 7-inch casing, while the second and third were applied using plug and perforation operations over two intervals in the casing above the open hole section.

Three 8-level, 3-component, high-temperature digital receiver strings with sonde spacing at 100 ft (30 m) were planned to be placed at string depths of around 6700 to 7500 feet in each of three deep vertical monitoring wells surrounding the toe of injector well 16A(78)-32. Sensor locations were designed to guide placement of the stimulation stages, and hence to guide placement of a subsequent parallel, production well 16B(78)-32 to be drilled for obtaining fracture flow connection with the initial injection well. Following redeployment of the 8-level, 3C strings, 2-level 3C analog seismic sensors were to be placed in the wells for long term seismicity monitoring. Copious seismicity was generated by each of the three stimulation stages, analysis of which is just beginning. The impact of high downhole temperatures on the seismic sensors was greater than anticipated, leading to only partial instrument performance during the stimulation time, and an inability to continue with longer-term post-stimulation monitoring. Nevertheless, enough good quality event locations were obtained to allow confirmation of stress conditions and to permit targeting of the planned producer well 16B(78)-32.

## 1. Introduction

The Utah FORGE (Frontier Observatory for Research in Geothermal Energy), located 20 miles northeast of Milford, Utah, is a field laboratory supported by the U.S. Department of Energy to develop technology for characterizing and creating Enhanced Geothermal System (EGS) reservoirs (Moore et al., 2021) (Figure 1). The ultimate goal of the FORGE project is to demonstrate to the public, stakeholders and the energy industry that EGS technologies have the potential to contribute significantly to future power generation. Efforts to date have centered on the drilling of an inclined deep well (16A(78)-32 (hereafter referred to as 16A) for performing injection-related experiments plus three deep vertical monitoring wells (58-32, 56-32 and 78B-32) surrounding the toe of 16A (Figure 2). All wells encountered temperatures exceeding 200$^{o}$C in their deeper reaches in dominantly granitic basement well below the alluvial cover. The wells show natural fracture patterns and stress field orientations similar to those observed to the east in the Mineral Mountains (Simmons et al., 2019, 2020).

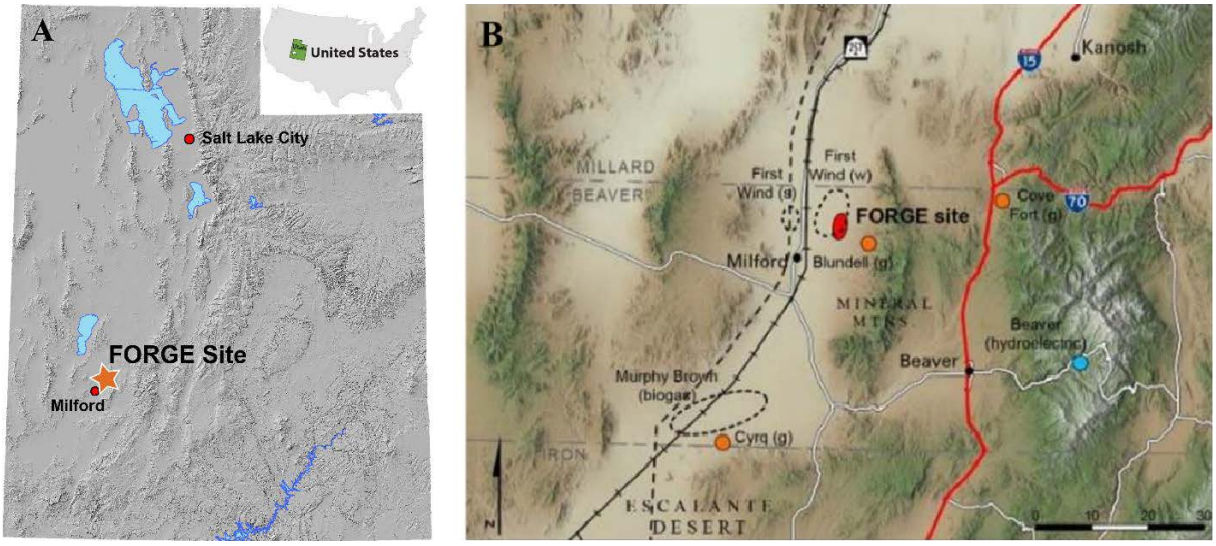


**Figure 1: Location maps of the Utah FORGE site. A) Map of Utah. B) Renewable energy projects in the region surrounding the FORGE site. Orange circles and (g) mark the locations of geothermal plants at Cove Fort (ENEL Green Power), Roosevelt Springs (Blundell Power Plant, PacifiCorp) and Thermo (Cyrq Energy). Dashed ellipses show the locations of other renewable energy projects. Graphic after Wannamaker et al (2021).**

The core goal of EGS involves the creation of sustainable rock permeability to extract heat for long periods of time. At Utah FORGE, hydraulic stimulation near the toe of injector well 16A was conducted from April 16-23, 2022, in three successive stages. This was done to assess the ability to form a (thermal) reservoir, confirm the stress regime, and to help guide placement of a later parallel test producer, 16B(78)-32, for achieving interwell flow. Seismicity induced by these stimulations needed to be monitored to map the EGS reservoir growth and to mitigate possible seismic hazards (Majer et al., 2016). An overview of the guiding risk studies, as well as the history of seismicity at the site and the planning and network deployed for monitoring potential seismic hazards is presented in Pankow et al. (2017, 2019).

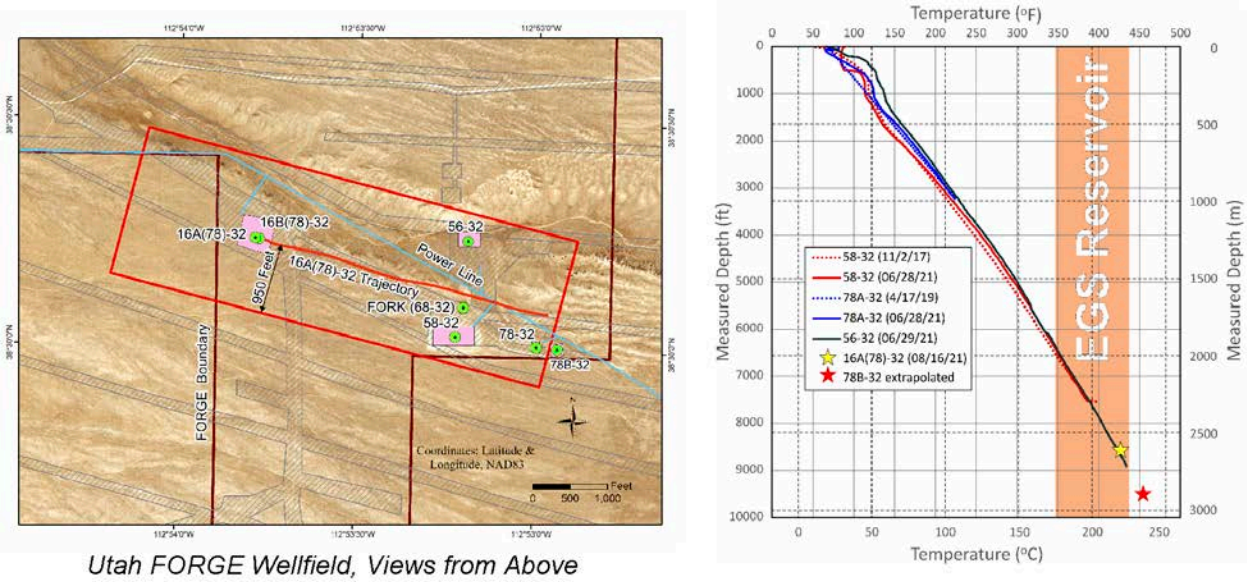


**Figure 2: Plan view of Utah FORGE wells. The treatment well is 16A(78)-32. The three deep vertical wells for placing high-temperature receiver strings are: 58-32, 56-32 and 78B-32.**

To assess reservoir zone characteristics and growth potential, monitoring was carried out using deep-borehole, multi-level, high-temperature receiver systems in three wells surrounding the toe of 16A (Figure 2). As designed, the borehole receiver systems were to provide continuous coverage through all injection operations, and post-stimulation flow testing, plus a shut-in period that may exceed one year following the initial stimulation tests. The downhole seismic array was intended to detect very small microseismic events ($-2.5 < M < -0.5$) for the purpose of mapping the stimulated fracture domains during and after the injection operations. During the stimulations, high-temperature, digital, eight-level (8L), three-component receiver strings (Geochains®) with separations of 100 ft, manufactured by Avalon Science Ltd (ASL), were deployed at or near reservoir depths. After injection, the digital strings in the three monitor wells were to be replaced with two-level retrievable, high-temperature 3C analog receivers separated by 1000 ft, also by ASL, for continuous long-term monitoring of reservoir microseismicity.

## 2. Synthetic Model Studies for Deployment Design

Estimates of microseismic location accuracies for a model 8L 3C array of 7500 ft maximum depth were computed using the method presented in Dyer et al. (2010). The computed errors for any given source location can be expressed as an error ellipsoid. The shape and orientations of these ellipsoids depends primarily on the combination of the arrival time data, the azimuthal or hodogram data, and the source-receiver geometries corresponding to each trial location in the model. Figure 3 shows the maximum errors in map and depth views for the case of three receiver strings placed deep within or near reservoir depths (Rutledge et al., 2021, 2022). The maximum error is the half-length of the error ellipsoid's principal axis. The horizontal slice (map view, Figure 3) is at a depth of 8500 feet corresponding to the TVD at the toe of 16A. The vertical slice

(depth view, Figure 3) corresponds to an east-west plane going through the toe of 16A (at north -1000 ft). Assumed crystalline velocities were Vp = 19000 ft/s and Vs = 11000 ft/s based on the deep well logs, with data accuracies of P picks of +/- 1 ms, S picks of +/- 2 ms, and hodogram azimuth accuracies of +/- 5°. Along most of the 16A lateral length, location uncertainties are of order 50 ft. If the maximum depth of the geophones is reduced to 5000 ft, uncertainties become of order 100 ft.

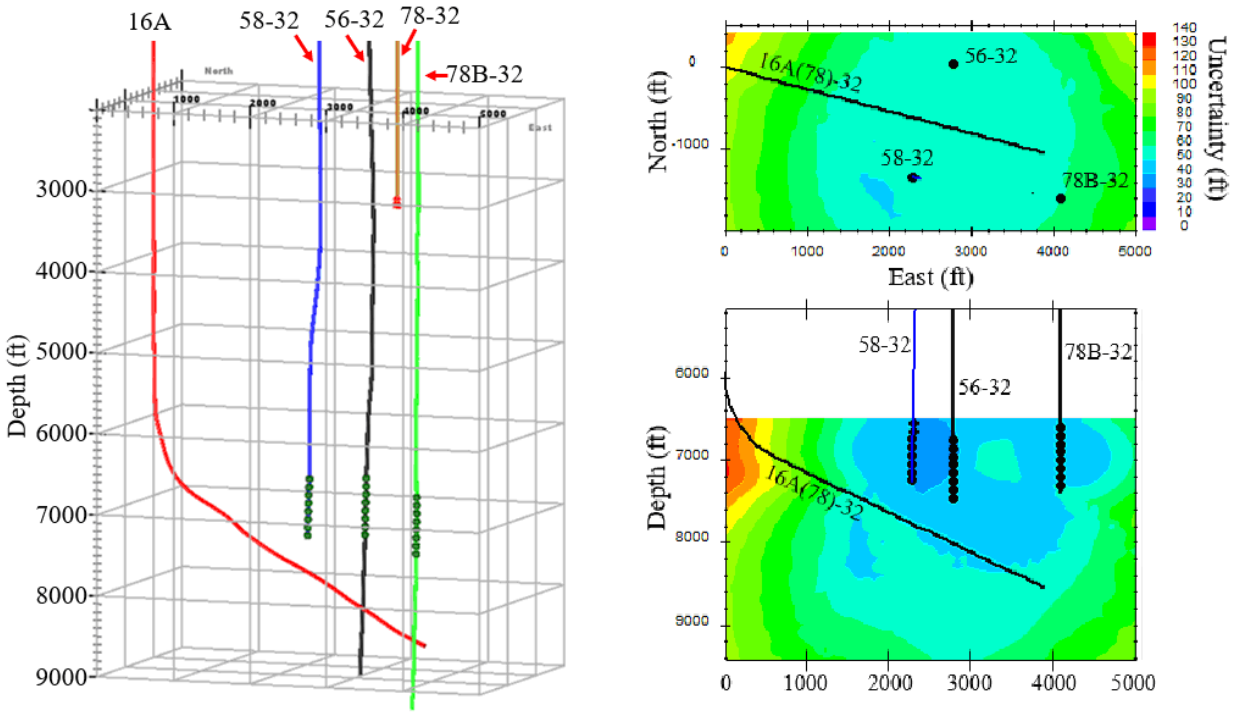


**Figure 3: Left: Perspective view of the treatment well 16A(78)-32 (abbreviated 16A) and the three deep wells 58-32, 56-32, and 78B-32, with the planned, deep receiver string placements shown as the green dots. The depth placements (7500 ft) are limited by the instrumentation's temperature specifications (~200°C). Right: Map and depth views of computed maximum uncertainties. The horizontal slice (map view) is at a depth of 8500 feet, close to the TVD of 16A. The vertical slice (depth view) corresponds to an east-west plane going through the toe of 16A (at north -1000 ft).**

A similar study of magnitude detections was performed using the method of Freudenreich et al. (2012). The S wave was used in this analysis because for real data it has better signal to noise ratio than the P wave and so may be expected to provide more reliable magnitudes. A seismic Q of 350 and a corner frequency of 120 Hz were determined by matching modelled sensitivities with the distribution of magnitudes of microseismicity observed in well 78-32 during the pilot injection tests in well 58-32 in April 2019 (Rutledge et al., 2021). For the 7500 ft deep receiver placement, detection thresholds over the toe target area of 16A should be down to about -2.2 to -2.3Mw for all receivers (Rutledge et al., 2021, 2022). Sensitivity was reduced to about -2.0Mw with the deepest sondes at only 5000 ft.

## 3. Deployment Sequence of Seismic Sensors During the 16A Stimulation

Stimulation operations began early on April 16, 2022 with a check shot using twelve, 21 gm Hero charges on a 2 ft long gun with 6 shots/ft and 60$^{o}$ phasing at measured depth of 10,826 ft in the open hole section of 16A. Unfortunately, only the 8L geophone string in 58-32 was locked and performing at that time with a depth of 6700 ft for the deepest sensor, whereas the strings in 56-32 and 78B-32 were not functioning. Attempts to deploy at greater depth led to sonde interior temperatures becoming too high for instrument performance. Maximum sonde interior temperature was 158$^{o}$C (stated rating was 165$^{o}$C), corresponding to an external temperature according to the well log of 181$^{o}$C (Figure 2). The check shot was detected on the string, and bulk velocities of Vp = 18700 and Vs = 10930 ft/s determined, which are close to the average borehole log values (19000 and 11,000 ft/s respectively) used in the prior model simulations. Geophone group orientations also were determined using the known location of the check shot. Subsequently, the first stimulation pumping stage began with rates up to 50 bpm for a total of 4261 bbl injected through the open hole section of 16A. Several thousand seismic events were induced in the region of the toe (Figure 4), preliminary analysis of which will be discussed.

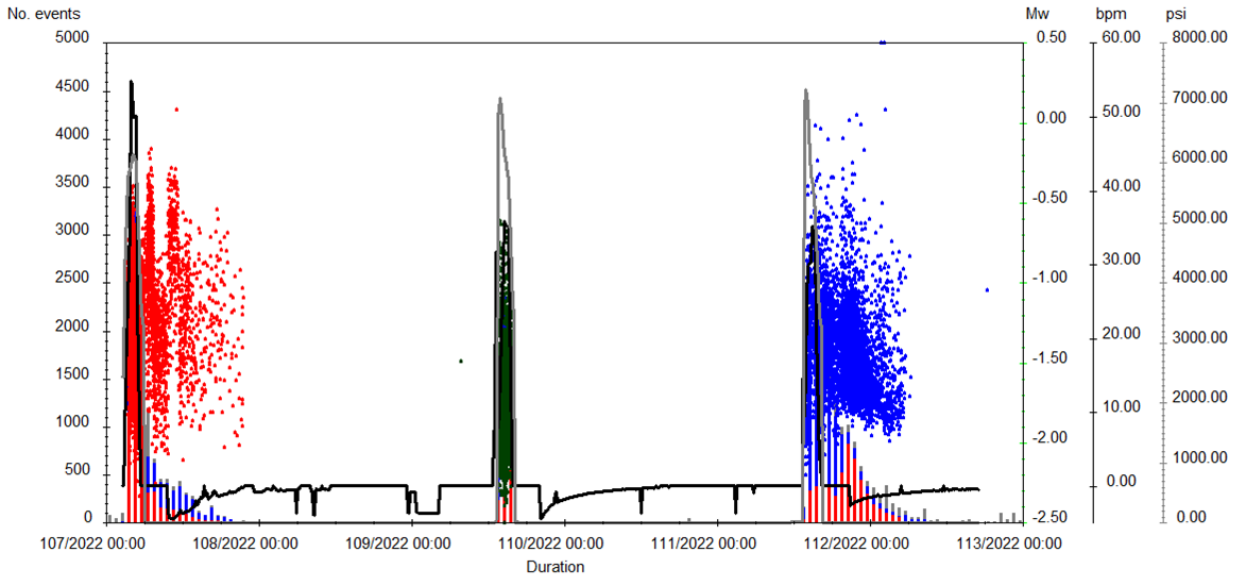


**Figure 4: Event rate histogram vs event magnitude, pump rate and injection pressure for the three stimulations of well 16A over the April 16-23, 2022, time frame. The grey curve is pressure (psi) and the black curve is injection rate (barrels per minute). In the histograms (number of events/hour), red is located events, blue is events that were not located and grey is noise triggers. Red, green and blue scatter plots are individual events giving an indication of magnitude. Dates are Julian. Note, this plot was generated in the field during the real time data acquisition; the abrupt halt in the event rate following the stage 2 stimulation is due to a 24 hour gap in the triggering, and is not real.**

The second stimulation stage began on April 18 midday with the setting of a bridge plug at a measured depth of 10665 ft, with plug integrity tested by holding surface pressure at 7042 psi. Stage-2 perforation shots were detonated similar to the check shot but using a 20 ft gun over the interval 10560-10580 ft, and 2770 bbl of friction-reduced freshwater was pumped through the perforated zone. Once more, several thousand seismic events were induced around the isolated

region which currently are being analyzed. The locked 8L geophone string in well 58-32 was functioning at that time. Attempts to have the geophone strings perform in 56-32 and 78B-32 were again not successful so, in well 56-32, the 8-level Geochain was replaced with a 2-level analog string with sondes at 7315 and 8315 ft depth respectively. The analog string's chemically triggered locking arms did not deploy in time for the second stimulation, but P and S first arrivals were recorded and will be incorporated later into the analysis.

After flowing back the second stage, a second bridge plug was set at a measured depth of 10460 ft. The third stimulation stage began early April 21, 2022, with similar perforations in the interval 10120-10140 ft, followed by 3016 barrels pumped, using a slickwater pad and then cross-linked CMHPG (carboxymethyl hydroxypropyl guar) along with small concentrations of micro-proppant. For this stage, a second 8L 3C seismic chain was operational in well 78B-32 with a maximum depth of 6200 ft. The maximum deployable depths of the chains were determined by keeping the maximum reported interior temperatures conservatively 10-15$^{o}$C below rating. In addition, the analog geophone pair deployed in well 56-32 continued to function and was by then fully locked, allowing full tri-well recording. Several thousand seismic events again were induced around the isolated region. In addition, the stimulation perforation shots fired before the third stage were recorded on all three wells' sensors (Figure 5) enabling sensor orientation and verifying the prior check shot velocity estimates in the reservoir zone.

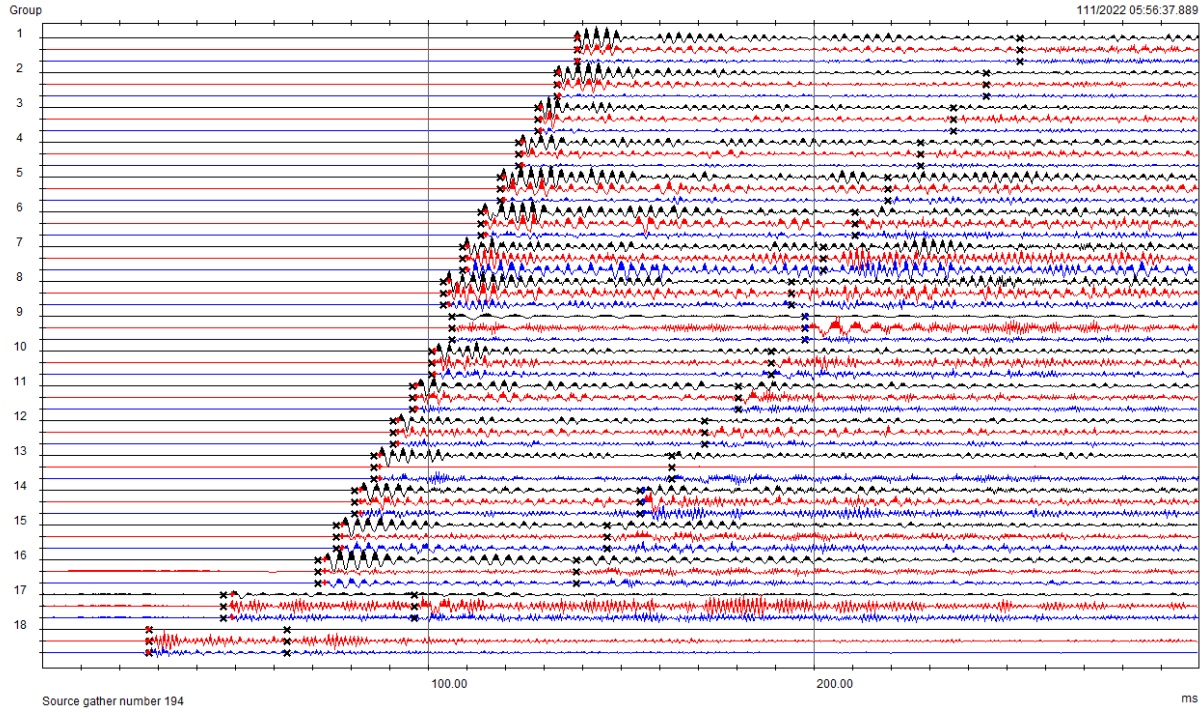


**Figure 5: Stage 3 perforation: 78B geophone string groups 1-8, 58 string groups 9-16 and 56 string groups 17 and 18. The good fit between the picked P times (red +) and the S arrivals to the model times (black x) of the third perforation shot demonstrates that the P and S velocities are reliable for the network of sensors in the three wells.**

Altogether, a total of 34,272 events triggered over the three stimulations. These were distributed as 13,314 in stage 1 (6,377 auto-locations), 4,438 in stage 2 (2,880 auto-locations) and 16,326 in stage 3 (5,382 auto-locations). The triggering used a waveform stacking technique to identify potential events from within the continuous trace data (Dyer, 2011). A trigger occurred when the sum of the rms trace amplitude of each 3C receiver group exceeded a threshold level when stacked at the P and S model times from any point within a 100 ft cubic search grid. The analog 2-level sonde in well 56-32 failed on the morning of April 22, illustrating our good fortune in having triwell function for the key time span of the third stimulation. Analog pairs subsequently deployed in 58-32 and 78B-32 also failed; consequently, long-term seismicity monitoring at reservoir depths did not go forward.

## 4. Event Location and Magnitude Results to Date for the 16A Stimulation

Not having all three deep vertical wells active with seismic monitoring instruments during the first two stimulation stages prevented good accuracy for real-time event auto-location. The auto-locations were performed in near real time using the stacking method of Dyer (2011) followed by magnitude estimation using a time domain technique (Wallace and Lay, 1995). Auto locations of stages 1 and 2 had a wide scatter of event locations due to the difficulty of obtaining reliable event azimuths automatically with a single geophone string. Hence, we concentrate here on preliminary results from the third stage where two of the digital and one of the analog strings were functioning.

A typical event from stage 3 with good signal to noise (-1.6Mw) is shown in Figure 6. The P and S picks, event location and magnitude for such events were all derived automatically. The largest visually checked event had a magnitude of 0.2Mw on 24th April (day 114) at 11:44:15 (Figure 7). This is two days after the third stimulation and beyond the time duration of the event rate display of Figure 4. It also occurred after the PSS analog seismometer pair in well 56-32 ceased working.

During stage 3, the network of sensor strings in 56, 58 and 78B provided reasonable event locations distributed predominantly NNE-SSW through the stage 3 perforation location (Figure 8). The real time monitoring of this stage consisted of visually checking each auto location and removing those that did not have a good fit between the model times and the P/S arrivals. The outliers in the distribution also were checked to reduce the potential for misinterpretation of spurious features. The preliminary distribution of events processed in the field (Figure 8) is parallel to the maximum principal stress orientation of NNE/SSW determined for the FORGE project area and the neighboring Mineral Mountains (Moore et al., 2020). The seismic events also grew predominantly upwards in relation to the stimulation zones. These trends are consistent with pseudo radial growth of a relatively simple fracture system in the background stress field. The minimum recorded magnitude was -2.3Mw, and the maximum was 0.2Mw occurring after the time window of Figure 4. Treatment pressures measured during this third fracturing stage (and in the second fracturing stage) are characterized by declining pressure that is also consistent with relatively planar, radial fracture growth (Miskimins, 2019). Future modeling efforts will history match these data to attempt to confirm this hypothesized fracture growth model.

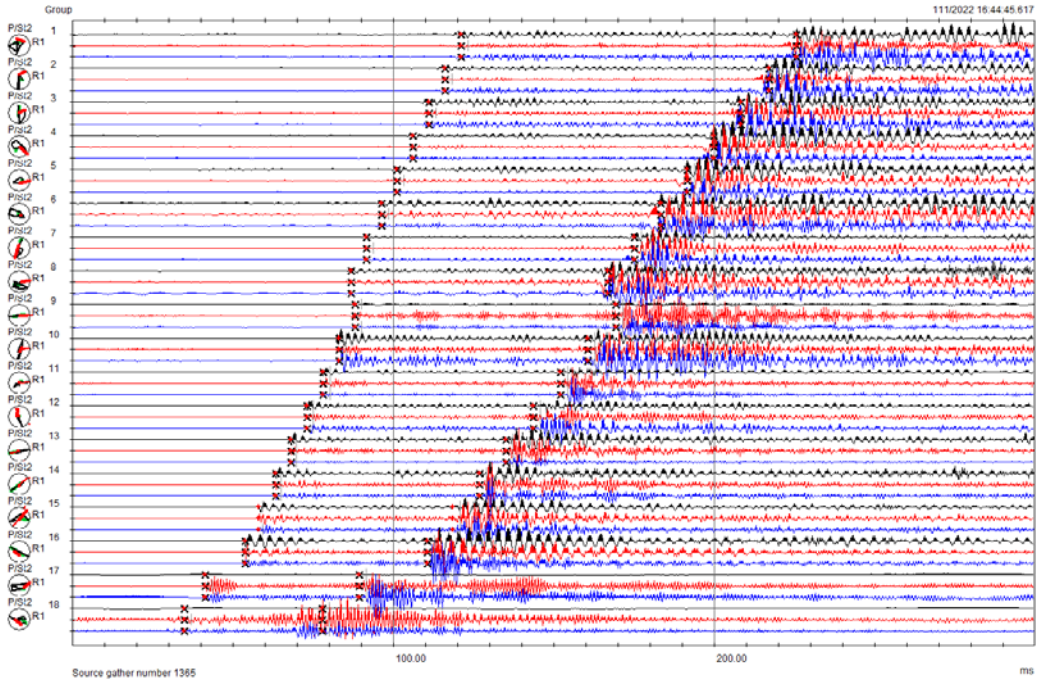


**Figure 6: Typical event from stage 3, -1.6Mw. 78B 3C string groups 1-8, 58 string groups 9-16 and 56 groups 17-18. Small circular plots along left side are hodograms (particle motions) of the red vs blue traces in each group.**

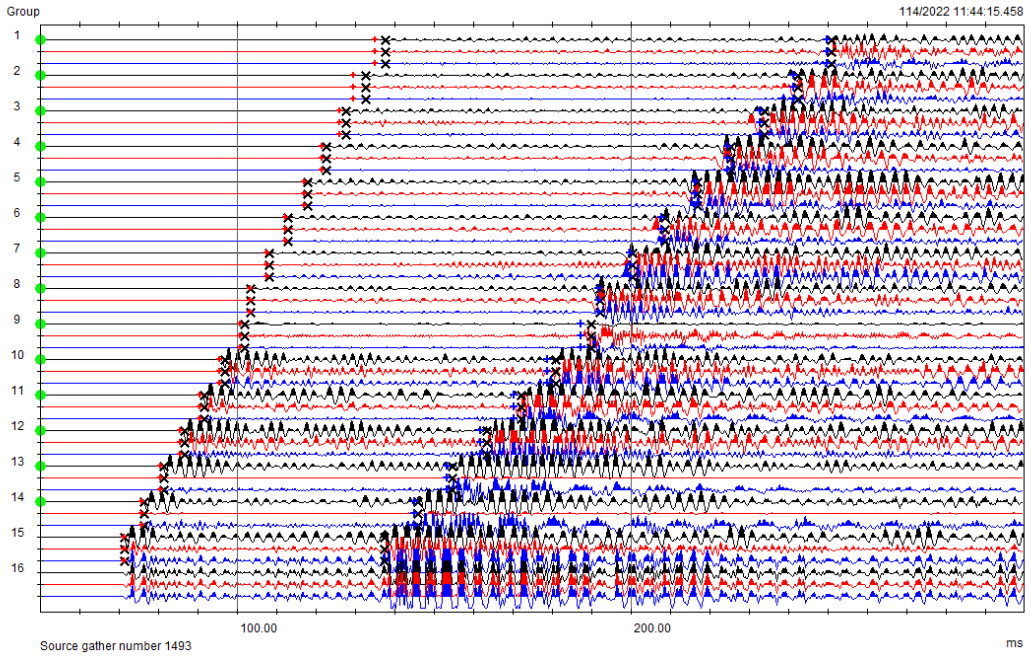


**Figure 7: Largest event, 0.2Mw detected after stage 3. 78B 3C string groups 1-8, 58 string groups 9-16. The PSS dual analog sonde in well 56 was not functioning at this time. The green disks at the start of the traces indicate that these groups were used in the auto-locater.**

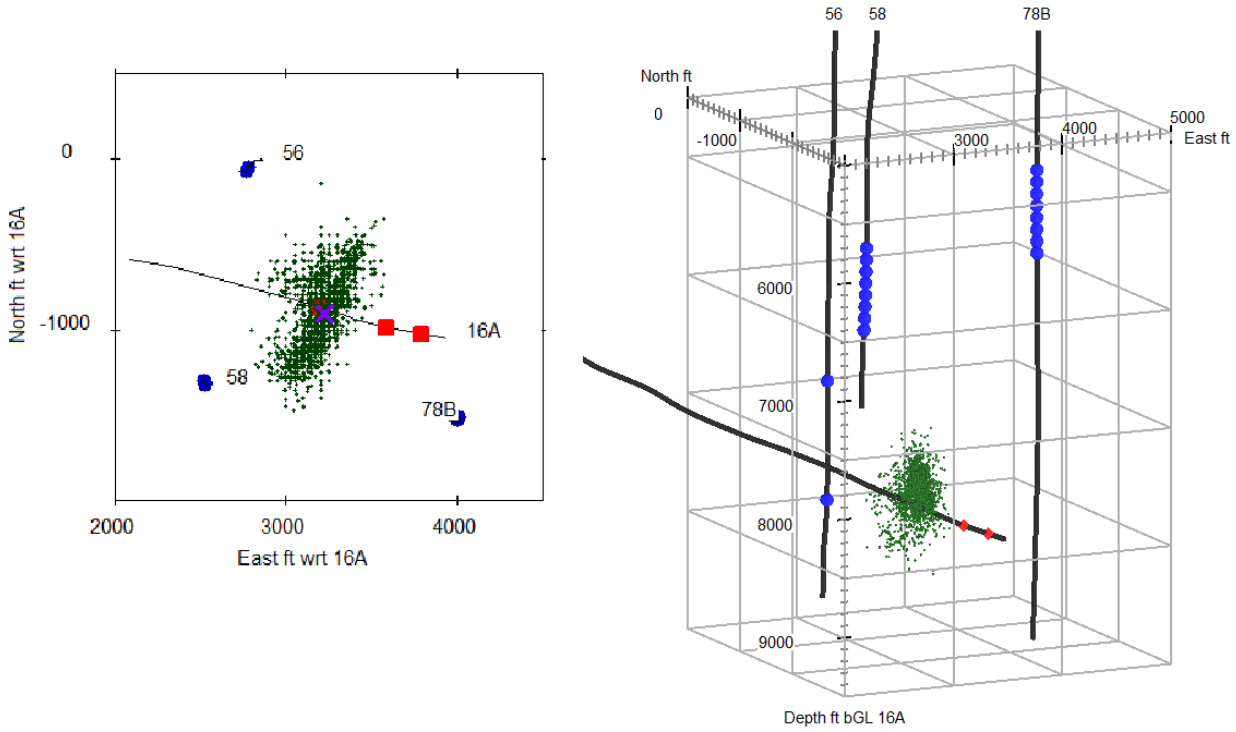


**Figure 8: Plan (left) and section view facing NNE (right) for the real-time microseismicity autolocations (green dots) during stage 3 of the injection in well 16A. Red squares or diamonds denote the three stimulation stage locations, where stage 3 is the uppermost one.**

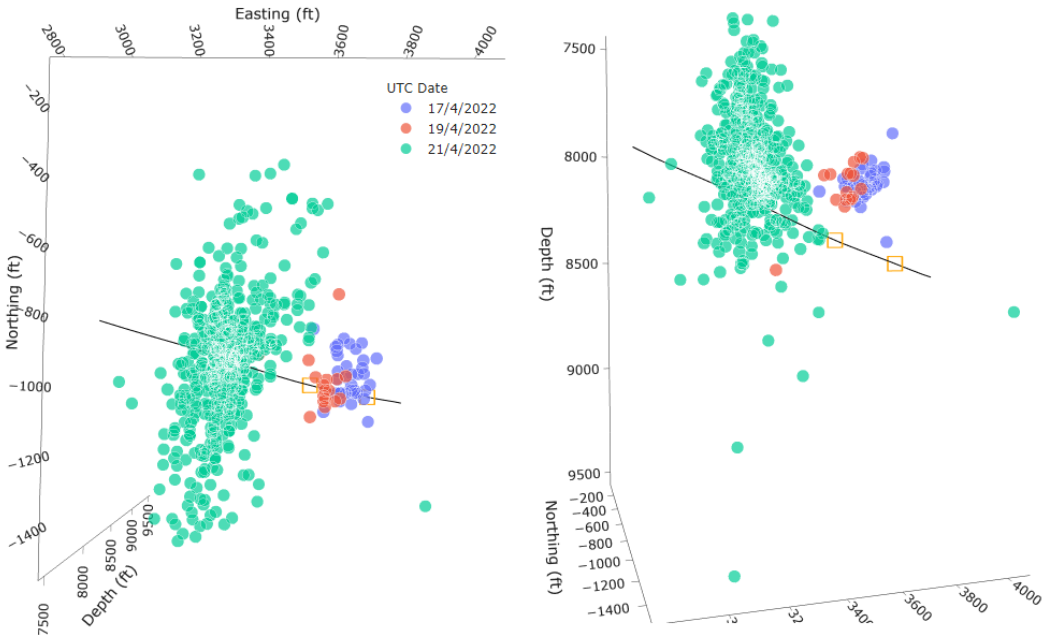


**Figure 9: Plan (left) and section view facing ~NNE (right) for the real-time microseismicity autolocations (green dots) during stage 3 of the injection in well 16A, together with preliminary manually picked events for stages 1 (purple dots) and 2 (red dots).**

Given the solitary real-time monitoring string in 58-32 during stimulation stages 1 and 2, those P and S travel times and P hodograms (e.g., Hendricks and Hearn, 1999) had to be picked manually. The events in these two stages shown here (Figure 9) were derived from relatively larger magnitude events by manually interpreting the hodograms and picking the P and S times for each location. Nevertheless, these very preliminary event results also lie mainly above the trajectory of injector well 16A, and the stage clusters appear to be separate. Any trend at present appears consistent with a NNE-SSW principal stress direction. Substantial effort remains to complete the identification and analysis of good quality seismic events and improve the event resolution from injection stages 1 and 2.

## 5. Conclusions

Downhole seismic monitoring of events associated with the three-stage stimulation of well 16A was successful with the recording of many thousands of microseisms including tri-well results. Analysis is ongoing but a large number of good locations and magnitudes is anticipated to be derived that will characterize the reservoir and guide the trajectory of upcoming well 16B. With only a single recorded event reaching 0.2Mw, seismicity also stayed well below the thresholds of the governing traffic light system in place, i.e., no more than 10 1.0Mw or 1 2.0Mw events in a 24 hr period within 3 km of the injection site (Utah FORGE, 2020; Pankow, 2022). Principal challenges for geothermal seismicity monitoring pertain to component performance in environments at 200$^{o}$C or higher temperature. Utah FORGE has made ground-breaking progress in obtaining good results and charting a path forward for EGS development in crystalline rocks. Continued research should be supported into sensitive seismic instrumentation, deployment cabling, and protocols that can perform robustly under geothermal conditions.

## Acknowledgement

Funding was provided by The U.S. Department of Energy's Office of Energy Efficiency and Renewable Energy (DOE EERE) Geothermal Technologies Office under Project DE-EE0007080 Enhanced Geothermal System Concept Testing and Development at the Milford City, Utah Frontier Observatory for Research in Geothermal Energy (FORGE) site. The microseismic data processing and some of the borehole sensors in this study were supported under the Haute-Sorne EGS project (Switzerland) that benefits from an exploration subsidy of the Swiss Federal Office of Energy (contract number MF-021-GEO-ERK), which is gratefully acknowledged. We thank Avalon Sciences Limited and Schlumberger Technology Corporation for their efforts and assistance in deploying the seismicity instrumentation downhole and recording the events during the stimulation experiment in well 16A(78)-32. We also thank numerous EGI staff for crucial in-field data logistics and coordination, in particular Aaron Becar, Clay Jones and Jon Rusho.

## REFERENCES

Dyer, B. C., U. Schanz, T. Spillmann, F. Ladner, and M. O. Haring "Application of microseismic multiplet analysis to the Basel geothermal reservoir stimulation events." *Geophysical Prospecting*, 58, 791–807 (2010).

Dyer, B. C. “Method of Detecting Seismic Events and a System for Performing the Same”. United Kingdom Patent No. GB 0711698.1. Patent granted 25/10/2011 (2011).

Freudenreich, Y., S. J. Oates, and W. Berlang "Microseismic feasibility studies – assessing the probability of success of monitoring projects." *Geophysical Prospecting*, 60, 1043–1053 (2012).

Hendrick, N., and S. Hearn “Polarisation analysis: What is it? Why do you need it? How do you do it?” *Exploration Geophysics*, 30, 177-190, doi: 10.1071/EG999177 (1999).

Majer, E., J. Nelson, A. Robertson-Tait, J. Savy, and I. Wong "Best practices for addressing induced seismicity associated with enhanced geothermal systems (EGS)." *Topical report, Lawrence Berkeley National Laboratory*, prepared at the direction of the Dept. of Energy Geothermal Technologies Program, April 8, 115 pp. (2016).

Miskimins, J. L. (editor in chief) "Hydraulic Fracturing: Fundamentals and Advancements." Society of Petroleum Engineers Monograph Series, 795 pp. (2019).

Moore, J., J. McLennan, K. Pankow, S. Simmons, R. Podgorney, P. Wannamaker, C. Jones, W. Rickard, and P. Xing “The Utah Frontier Observatory for Research in Geothermal Energy (FORGE): A laboratory for characterizing, creating and sustaining Enhanced Geothermal Systems” *Proc. 45th Workshop Geothermal Reservoir Engineering*, Stanford University, Stanford, CA, SGP-TR-216, 10 pp. (2020).

Moore, J., S. Simmons, J. McLennan, K. Pankow, P. Xing, C. Jones, A. Finnela, P. Wannamaker, and R. Podgorney, “Current activities at the Utah Frontier Observatory for Research in Geothermal Energy (FORGE): A laboratory for characterizing, creating and sustaining Enhanced Geothermal Systems.” *Geothermal Resources Council Transactions*, 45, 802-813 (2021).

Pankow, K. L., S. Potter, H. Zhang, and J. Moore “Local seismic monitoring at the Milford, Utah FORGE site.” *Geothermal Resources Council Transactions*, 41, 9 pp. (2017).

Pankow, K. L., S. Potter, H. Zhang, A. J. Trow, and A. S. Record "Micro-seismic characterization of the Utah FORGE site." in Allis, R., and Moore, J. N., editors, *Geothermal characteristics of the Roosevelt Hot Springs system and adjacent FORGE EGS site, Milford, Utah*: Utah Geological Survey Misc. Pub. 169-G, 10 pp. (2019).

Pankow, K., J. Rutledge, B. Dyer, R. Burlacu, P. Bradshaw, A. Dzubay, J. M. Hale, G. Petersen, J. A. Rusho, P. Wannamaker, K. Whidden, and J. Moore “Local seismic monitoring of a well stimulation at the Utah Frontier Observatory for Research in Geothermal Energy site.” *Abstract*, Annual Seismological Society of America Meeting, Bellevue, WA, April 10-23 (2022).

Rutledge, J., K. Pankow, B. Dyer, P. Wannamaker, P. Meier, F. Bethmann and J. Moore. "Seismic monitoring at the Utah FORGE EGS site." *Geothermal Resources Council Transactions*, 45, 13 pp. (2021).

Rutledge, J., B. Dyer, F. Bethmann, P. Meier, K. Pankow, P. Wannamaker, and J. Moore "Downhole microseismic monitoring of injection stimulations at the Utah FORGE EGS site." *Extended abstract, American Rock Mechanics Association annual meeting*, Santa Fe, 5 pp. (2022).

Simmons, S. F., S. Kirby, R. Bartley, A. Allis, E. Kleber, T. Knudsen, J. J. Miller, C. Hardwick, K. Rahilly, T. Fischer, C. Jones, and J. Moore “Update on the geoscientific understanding of the Utah FORGE site.” *Proc. 44th Workshop on Geothermal Reservoir Engineering*, Stanford University, Stanford, CA, SGP-TR-214, 10 pp. (2019).

Simmons, S., R. Allis, S. Kirby, J. Moore “Production chemistry evidence for an EGS type reservoir in Roosevelt Hot Springs and implications for Utah FORGE.” *Proc. 45th Workshop on Geothermal Reservoir Engineering*, Stanford University, Stanford, CA, SGP-TR-216, 10 pp. (2020).

Utah FORGE. “Utah FORGE Induced Seismicity Mitigation Plan: Enhanced Geothermal System Testing and Development at the Milford, Utah FORGE Site”, https://gdr.openei.org/submissions/1319 (2020).

Wannamaker, P., V. Maris, K. Mendoza and J. Moore. "Deep heat and fluid sources for the Roosevelt Hot Springs hydrothermal system and potential heat for the Utah FORGE EGS from 3D FORGE and SubTER magnetotelluric coverage." *Geothermal Resources Council Transactions*, 45, 847-863 (2021).

Wallace, T. C. and T. Lay “Modern global seismology.” Academic Press International Geophysics Series, 521 pp. (1995).